

Article

Changes in Reference Evapotranspiration and Its Contributing Factors in Jiangsu, a Major Economic and Agricultural Province of Eastern China

Ronghao Chu ^{1,†} , Meng Li ^{1,†}, Shuanghe Shen ^{1,*}, Abu Reza Md. Towfiqul Islam ^{1,2} ,
Wen Cao ³ , Sulin Tao ¹  and Ping Gao ⁴

¹ Collaborative Innovation Center on Forecast and Evaluation of Meteorological Disasters, Jiangsu Key Laboratory of Agricultural Meteorology, School of Applied Meteorology, Nanjing University of Information Science & Technology, Nanjing 210044, China; ronghao_chu@163.com (R.C.); lm_nuist@163.com (M.L.); gm_towfique_06@yahoo.com (A.R.M.T.I.); sulin.tao@outlook.com (S.T.)

² Department of Disaster Management, Begum Rokeya University, Rangpur 5400, Bangladesh

³ Anhui Meteorological Institute, Anhui Province Atmospheric Science and Satellite Remote Sensing Key Laboratory, Hefei 230031, China; sgfxxy_0@163.com

⁴ Meteorological Service Centre for Jiangsu Province, Nanjing 210008, China; gaoping5268@126.com

* Correspondence: yqzhr@nuist.edu.cn; Tel.: +86-25-5873-1011

† These authors contributed equally to this work.

Received: 10 April 2017; Accepted: 30 June 2017; Published: 2 July 2017

Abstract: Reference evapotranspiration (ET_{ref}) is a key parameter of hydro-meteorological studies as well as water resource planning. In this study, we adopted the Penman–Monteith FAO 56 model to estimate ET_{ref} and through the differential equation and detrending method to determine sensitivities and the contributions of four meteorological parameters to ET_{ref} based on daily weather data from 60 stations of Jiangsu province during 1961–2015. Results reveal that ET_{ref} and its trends in the three sub-regions of the Jiangsu province had a significant spatial heterogeneity. A significant decreasing tendency of ET_{ref} ($p < 0.001$) was observed in the Huaibei region, while a slightly increasing tendency was identified in the Jianghuai and Sunan regions. These changes of ET_{ref} were caused by a significant increasing trend in air temperature (TA) and significant decreasing trends in wind speed (WS), sunshine duration (SD) as well as a non-significant change trend in actual vapor pressure (VP). However, the VP was the meteorological parameter to which ET_{ref} was most sensitive, whereas ET_{ref} was more sensitive to TA and SD in the summer but less so in the winter; the least sensitive factor, WS , had the opposite trend. Across the whole region, WS contributed most to ET_{ref} , followed by SD , while the positive contribution of TA to ET_{ref} could not offset the negative contributions of WS and SD . Although the effect of VP on changes in ET_{ref} is small, it could not be ignored, especially in the winter. The reverse relationship between increasing TA and decreasing ET_{ref} , namely the “evaporation paradox,” occurred in Jiangsu province. Thus, the outcomes of this study will contribute to thorough insight into the response to changes in ET_{ref} to the provincial water planning and management in eastern China.

Keywords: reference evapotranspiration; sensitivity coefficient; contribution; evaporation paradox; Jiangsu province; eastern China

1. Introduction

Reference evapotranspiration (ET_{ref}) plays a vital role in climatological and hydrological researches, where spatial and temporal variations are a key indicator of changing climate and water resource allocation [1,2]. The study of spatial and temporal changes of ET_{ref} has drawn much attention

in recent decades to regional-scale hydro-climatic change because of its nexus in the water resource management and terrestrial ecosystems [3–6]. Additionally, ET_{ref} not only plays a role in estimating agricultural water requirements, but also in irrigation scheduling and management [7]. Therefore, knowledge into the changes of ET_{ref} and its precise estimation responses to climate change conditions has become more important ever [8,9], particularly in the context of climate warming starting in the 1970s [10].

Meteorological factors and ET_{ref} have changed drastically in the recent decade, due to the anthropogenic activities and land use changes [11–13]. In the last century, mean air temperature has risen by 0.6 °C globally on average, and mean temperature has also increased by 0.5–0.8 °C in China [10]. Despite an increasing trend in the air temperature, a significant number of works have found decreasing pan evaporation and ET_{ref} in many parts of the world, including China [14–16], Australia [17], New Zealand [18], Canada [3], India [19], Thailand [20], and Mexico [21]. This has led to the coinage of the term “evaporation paradox” introduced by Brutsaert and Parlange [22]. However, the reason for its occurrence is still debatable [23]. Hobbins et al. [24] showed that the pan evaporation paradox is an indicator of the close linkage between actual evaporation and potential evaporation. Meanwhile, other researchers have also reported some strong proofs in accordance with the opinion of Hobbins et al. [24] that decreasing rates of ET_{ref} are responsible not only for the rise in air temperature but also for other meteorological factors such as the reduction in wind speed, solar radiation, and relative humidity [25,26].

The Penman–Monteith FAO 56 model suggested by the Food and Agriculture Organization (FAO) has been regarded as a robust and universally accepted method for calculating ET_{ref} [27,28]. From the Penman–Monteith method, it is evident that most climatic parameters are affected by ET_{ref} , including air temperature, wind speed, relative humidity, and sunshine duration, as well as net radiation. In addition, various attribution analysis techniques have been applied to determine the contribution of climatic factors on ET_{ref} changes. The most widely used technique is a sensitivity coefficient analysis, which has been employed to measure the changes of ET_{ref} in response to an observed change of climatic parameters [23,29]. However, this method does not investigate the evaporative process, but only shows the relative contributions of climatic factors on ET_{ref} changes. Xu et al. [8] have developed a technique for analyzing the relative change of evaporation demand through statistical and mathematical modeling. This mathematical approach has been commonly used to calculate the relative changes in ET_{ref} analysis. For instance, Xu et al. [8], Li et al. [30], Liu et al. [31], and Huo et al. [32] used this technique for an attribution analysis of change in ET_{ref} in different regions of China. Similarly, in the present study, we successfully apply this technique to Jiangsu province in eastern China.

However, Liu et al. [15] showed a reverse relationship between rising temperature and reducing evaporation in southwest China, which appeared to represent a paradoxical situation and decreases the contribution of wind speed to the ET_{ref} changes to compensate for the increased contribution of mean air temperature. Wang et al. [23] found that the contributions of solar radiation, wind speed, and relative humidity are the major driving factors for the decrease in ET_{ref} for the three-river source region of China. Hence, further evaluation is essential to determine the relationship between climatic factors that causes changes in ET_{ref} in Jiangsu province. Attribution analysis of changes in ET_{ref} will involve a detrending method that will be discussed in detail in this study.

Evapotranspiration (ET), an important climatic parameter that mainly controls the water balance process, has a great impact on hydro-meteorology processes under a changing climate [33,34]. In water-limited regions, changes in ET_{ref} will be the result of changes in ET (and so the water balance), whereas in energy-limited regions they drive changes in ET. The change of ET_{ref} is a key component of hydro-meteorological studies in Jiangsu province. Several regional studies have documented the ET_{ref} in the Yangtze River basin [8,35,36]. Furthermore, a few studies have assessed the spatial distribution and temporal changes in the ET_{ref} trends and its magnitude and spatial patterns of ET_{ref} trends in eastern China. However, so far, changes in ET_{ref} and its contributing factors in Jiangsu province have yet to be investigated thoroughly, and the province is located in the Yangtze River

Delta, which contributes to the highest GDP in economy and is an emerging developed region. As an important economic province, Jiangsu also ranks at the top in terms of agricultural systems in China. This province has distinctive monsoon climatic characteristics, which makes it inherently sensitive to climate change [37]. It is therefore important to investigate changes in ET_{ref} trends and its contributing factors, which can provide a theoretical basis and scientific guidance for the management and allocation of water resources in Jiangsu province. The goals of this study are to explore the spatial–temporal trends in ET_{ref} in the Jiangsu province based on weather data from 60 stations during 1961–2015, and to estimate sensitivities and contributing factors to changes in ET_{ref} through a detrending method applied to the Penman–Monteith FAO 56 model. It is anticipated that the outcomes of this study will provide better guidance for agricultural production and economic development in this vital region.

2. Materials and Methods

2.1. Study Area and Data Source

Jiangsu province is located on the eastern coast of China and at the lower reaches of the Yangtze River and Huai River, which across its south and north, respectively, cover an area of $1.03 \times 10^5 \text{ km}^2$. The terrain primarily consists of plains, including the southern Jiangsu plain (south of Yangtze River), the middle Jianghuai plain (between Yangtze River and Huai River) and the northern Huang-Huai plain (north of Huai River), which comprises about 70% of the provincial area (Figure 1). The study area belongs to the East Asian monsoon zone and the transition between a subtropical zone and a warm temperate zone, which has distinct monsoon climate characteristics. Generally, the large area of the southern Huai River belongs to subtropical humid monsoon climate, the northern area belongs to temperate semi-humid monsoon climate [38]. There is a clear discrepancy between four seasons, the sunshine duration is 2000~2600 h, mean temperature is 13~16 °C, the frost-free period is about 200~240 days, and mean precipitation is 800 mm~1200 mm on an annual scale, with more than 60% of rainfall occurring during the summer season [39].

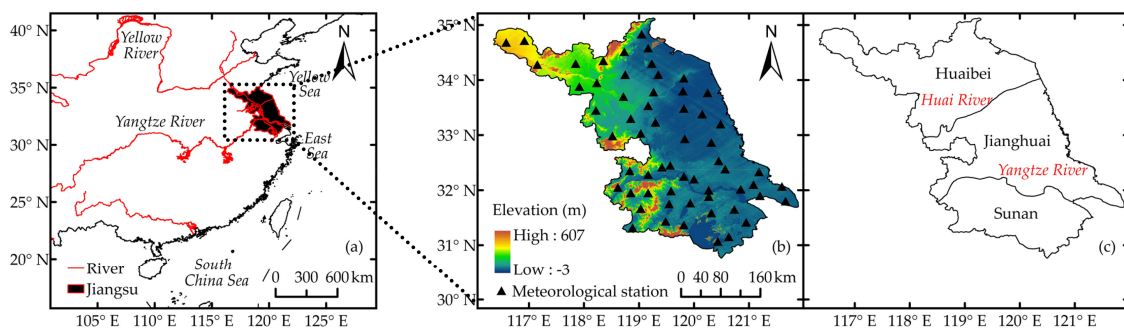


Figure 1. Map showing Jiangsu province: (a) location; (b) meteorological station (▲) and elevation; (c) sub-regions and rivers.

The locations of meteorological stations and the elevation are shown in Figure 1. The Jiangsu Province is divided into Huaibei, Jianghuai, and Sunan regions on the basis of two major rivers (Huai River and Yangtze River) and their regional climate characteristics. The basic climatic characteristics of the three sub-regions and the whole Jiangsu province are shown in Table 1. As seen from Table 1, the annual mean temperature (15.09 °C), the mean relative humidity (76.15%), wind speed ($2.79 \text{ m}\cdot\text{s}^{-1}$), sunshine duration (2116.07 h), and annual reference evapotranspiration (892.24 mm) have been observed for the last 55 years (1961–2015) in the whole of Jiangsu province.

Table 1. Basic climatic characteristics of three sub-regions and the whole of Jiangsu province during 1961–2015.

Region	TA (°C)	RH (%)	WS (m·s ⁻¹)	SD (h)	ET _{ref} (mm)
HuaiBei	14.30	72.96	2.54	2250.34	898.66
Jianghuai	15.15	77.41	2.94	2098.33	883.72
Sunan	15.94	77.71	2.85	1986.46	899.74
Whole	15.09	76.15	2.79	2116.07	892.24

Ground-based daily meteorological data from 60 meteorological stations provided by the Jiangsu Meteorological Information Centre (JMIC) of the China Meteorological Administration (CMA) including the daily mean temperature (T , °C), maximum temperature (T_{\max} , °C) and minimum temperature (T_{\min} , °C), precipitation (P , mm), sunshine duration (SD , h), wind speed (WS , m·s⁻¹) at 10 m height, and relative humidity (RH, %) during 1961–2015. The station dataset is checked by the JMIC. In addition, this study has performed routine quality checks and error correction for data following the techniques defined by Peterson et al. [40]. The four seasons are spring (March–May), summer (June–August), autumn (September–November), and winter (December–February of the next year).

2.2. Penman–Monteith FAO 56 Model for ET_{ref} Estimation

The Penman–Monteith FAO 56 model is a broadly accepted method for estimating ET_{ref} suggested by the Food and Agriculture Organization (FAO) of the United Nations [27]. The method employed in this study because it is physically based and integrates physiological characteristics and aerodynamic variables. According to the Penman–Monteith FAO 56 model, the ET_{ref} is estimated by the following:

$$ET_{ref} = \frac{0.408\Delta(R_n - G) + \gamma \frac{900}{(T+273)} u_2 (e_s - e_a)}{\Delta + \gamma(1 + 0.34u_2)}, \quad (1)$$

where ET_{ref} is the reference crop evapotranspiration (mm·d⁻¹), Δ is the slope of temperature variation with saturated vapor pressure (kPa·°C⁻¹), R_n is the net solar radiation flux (MJ·m⁻²·d⁻¹), and G is the soil heat flux density (MJ·m⁻²·d⁻¹), which is negligible relative to R_n , especially for vegetated coverage and at daily time steps, thus it may be ignored and $G = 0$. γ is a psychrometric constant (kPa·°C⁻¹), T is the daily mean air temperature (°C), u_2 is the wind speed at 2 m height (m·s⁻¹), e_s is the saturation vapor pressure (kPa), and e_a is the actual vapor pressure (kPa).

For the calculation of ET_{ref} , wind speed at 2 m height can be converted from the wind speed measured at 10 m based on the Penman–Monteith FAO 56 model as follows:

$$u_2 = u_z \frac{4.87}{\ln(67.8z - 5.42)}, \quad (2)$$

where z is the measured height above the ground surface (m) and u_2 and u_z are the wind speed at 2 and z meters height, respectively.

In this study, the total net solar radiation in the background is estimated based on the measured data of sunshine duration, combined with the Angstrom formula [41], which is given below:

$$R_s = (a_s + b_s \frac{n}{N}) R_a, \quad (3)$$

where R_s is the daily total solar radiation reaching the ground (MJ·m⁻²·d⁻¹), n is the daily measured sunshine duration hours (h), N is the greatest possible sunshine duration hours (h), R_a is the extraterrestrial solar radiation (MJ·m⁻²·d⁻¹), and a_s and b_s are the regression coefficients—according

to Chen et al. [42], the values were set to 0.19 and 0.53, respectively. Equations (4)–(6) are used to estimate incoming shortwave and outgoing long-wave radiation:

$$R_{ns} = (1 - \alpha)R_s \quad (4)$$

$$R_n = R_{ns} - R_{nl} \quad (5)$$

$$R_{nl} = \sigma \left(\frac{T_{\max,K}^4 + T_{\min,K}^4}{2} \right) (0.34 - 0.14\sqrt{ea}) \left(1.35 \frac{R_s}{R_{so}} - 0.35 \right), \quad (6)$$

where R_{ns} is the net incoming shortwave radiation ($\text{MJ} \cdot \text{m}^{-2} \cdot \text{d}^{-1}$), α ($=0.23$) is the albedo of the reference grassland, R_{nl} is the net outgoing long wave radiation ($\text{MJ} \cdot \text{m}^{-2} \cdot \text{d}^{-1}$), σ is the Stefan–Boltzmann constant ($=4.903 \times 10^{-9} \text{ MJ} \cdot \text{K}^{-4} \cdot \text{m}^{-2} \cdot \text{d}^{-1}$), R_{so} is the calculated clear-sky radiation ($\text{MJ} \cdot \text{m}^{-2} \cdot \text{d}^{-1}$), and R_s/R_{so} is the relative shortwave radiation. Detailed calculation procedures can be found in Chapter 3 of the FAO Irrigation and Drainage paper No. 56 [27].

2.3. Statistical Test for Trend Analysis

The Mann–Kendall (MK) statistical test [43,44] is a rank-based nonparametric method that has been extensively applied to the analysis of trends in reference evapotranspiration and related meteorological factors in hydro-meteorological time series data. One advantage of this MK test is that the dataset does not require the underlying data to follow a specific distribution. It can handle non-normality, missing values, or seasonality and is reliable for biased variables [45,46]. A nonparametric MK test was employed to show the trend variation in annual and seasonal ET_{ref} for each region in this study. Positive (negative) normalized Z values from the MK test indicate rising (declining) trends, respectively. An absolute Z value of the MK test exceeding 1.96 indicates that ET_{ref} has a significant change trend at the 95% confidence level, while an extremely noteworthy change trend was identified at the 99% significant level for the absolute Z value of the MK test more than 2.56. Additionally, to identify whether a trend exists, the Theil–Sen slope estimator developed by Sen [47] was used to determine the extent of a trend. This technique has been generally applied to detect the slope of a trend line in a hydro-meteorological time series dataset [48].

2.4. Spatial Interpolation Method for ET_{ref}

The IDW (Inverse Distance Weighted), a simpler numerical method, was used to investigate the spatial distribution of ET_{ref} in Jiangsu province. It has been widely applied to the spatial interpolation of climatic and hydrological point data like ET_{ref} [49], as well as rainfall [50]. Among various interpolation techniques, the IDW method was employed for the spatial distribution in the present study due to its easiness and estimated accuracy in comparison with other interpolation models like kriging. So we calculated the annual average estimated ET_{ref} at each station and then spatially interpolated it. All spatial interpolations were accomplished using ArcGIS 9.3 software (Environmental Systems Research Institute (ESRI), Redlands, CA, USA). The justification for using the IDW method is that this technique can compute the spatially interpolated values very fast and accurately.

2.5. Calculation of Sensitivity Coefficient

To identify the sensitivity of ET_{ref} related to climatic factors, a mathematically based sensitivity coefficient proposed by McCuen [29] in 1974 was applied in this study. Equation (7) is used to calculate the sensitivity of ET_{ref} as a mathematical basis:

$$S(v_i) = \lim_{\Delta v_i/v_i} \left(\frac{\Delta ET_{ref}/ET_{ref}}{\Delta v_i/v_i} \right) = \frac{\partial ET_{ref}}{\partial v_i} \times \frac{v_i}{ET_{ref}}, \quad (7)$$

where $S(v_i)$ is the non-dimensional sensitivity coefficient of ET_{ref} with respect to the climate variable (v_i). Positive (negative) sensitivity coefficients indicate that ET_{ref} increases or decreases with increases

in the climate variable v_i (where v_i is TA , VP , WS or SD). The absolute value measures the effect a given climate variable has on ET_{ref} . $\partial ET_{ref} / \partial v_i$ was calculated by partial differentiation of Equation (1); the detailed calculations can be found in the appendix of this paper.

2.6. Detrending Method

To evaluate the contributions of key meteorological factors to the change trend of ET_{ref} quantitatively, the detrending method, a statistical and mathematical operation of removing trend from the series, was employed in this study [8,30,31]. This is a simple but effective method. The main step of this method calculated by simple linear regression is demonstrated as follows:

$$\hat{g}_t = \hat{b}t + \hat{a}, \quad (8)$$

where \hat{b} and \hat{a} are the fitted linear regression coefficient and constant, respectively. \hat{g}_t is the fitted trend in time t . Then we removed the trend by subtracting the value of the trend line from the original data. Furthermore, to avoid negative values (e.g., VP , WS , and SD), the detrended dataset is currently defined as below:

$$y_t = x_t - \hat{g}_t + \hat{g}_1, \quad (9)$$

where x_t is the original time series of meteorological factors, \hat{g}_1 , corresponds to the first value of \hat{g}_t , and y_t is the ultimate detrended time series.

After removing the change trend in key meteorological factors, recalculating the ET_{ref} by using the detrended data series of one stationary meteorological factor and using the original data of remaining variables, comparing the recalculated ET_{ref} with the original value, the difference between them is identified as the contributions of that variable to the change trend of ET_{ref} . In order to quantify the contribution, an assessment index R is used to calculate by the following:

$$R = \sum_{i=1}^n \frac{ET_0^i - ET_0^R i}{ET_0^i}, \quad (10)$$

where ET_0^i and ET_0^R represent the original and recalculated ET_{ref} , respectively. n denotes the length of the time series. The larger the absolute value of R , the greater the contribution of that meteorological variable to the change trend of ET_{ref} . $R > 0$, $R < 0$ and $R = 0$ indicate that the trend in that meteorological variable has a positive, negative, or no contribution to the trend in ET_{ref} , respectively.

3. Results

3.1. Spatial Distribution of Seasonal and Annual ET_{ref}

Different spatial distributions of seasonal and annual ET_{ref} are shown in Figure 2. The ET_{ref} was higher in summer (335 mm~381 mm), followed by spring (221 mm~297 mm), autumn (176 mm~221 mm), and winter (85 mm~105 mm). The mean annual ET_{ref} over the whole Jiangsu province was about 892 mm during 1961–2015 (Table 1). In spring, the highest value was found in the Huaibei region. However, in the summer season, the spatial distribution of ET_{ref} showed a discrepancy, where the highest values were noticed in the Sunan region. Compared to the two seasons like autumn and winter, which had a similar spatial distribution of ET_{ref} , the higher value was observed in the southeast part of Jiangsu province (Sunan and Jianghuai region). In general, the annual spatial distribution of ET_{ref} had a relatively high value in northwest and south parts and low value in the central part of Jiangsu province (Figure 2a).

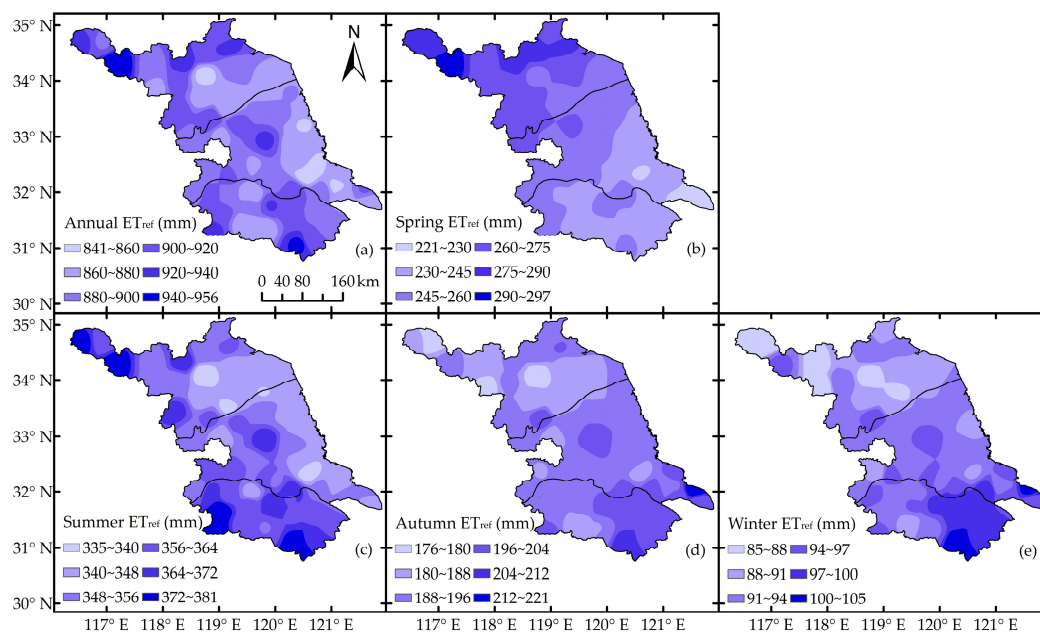


Figure 2. Spatial distribution of seasonal and annual ET_{ref} in Jiangsu Province during 1961–2015. Note: (a)–(e) represent ET_{ref} in annual, spring, summer, autumn, and winter seasons respectively.

3.2. Temporal Trends in Seasonal ET_{ref} and Climatic Factors

Table 2 presents the results of temporal trend for ET_{ref} . On the annual scale, the ET_{ref} values showed a slightly insignificant decreasing trend ($-0.245 \text{ mm}\cdot\text{a}^{-2}$) in the whole of Jiangsu province. A significant decreasing tendency (at 99.9% confidence level) was identified in the Huaibei region ($-1.468 \text{ mm}\cdot\text{a}^{-2}$), whereas a slightly increasing trend of ET_{ref} was observed in the Jianghuai ($0.207 \text{ mm}\cdot\text{a}^{-2}$) and Sunan ($0.592 \text{ mm}\cdot\text{a}^{-2}$) regions.

Table 2. Temporal trends for seasonal and annual ET_{ref} ($\text{mm}\cdot\text{a}^{-2}$) in each region of Jiangsu province from 1961 to 2015.

Region	Spring		Summer		Autumn		Winter		Annual	
	β	Z	β	Z	β	Z	β	Z	β	Z
Huaibei	0.039	0.09	-1.093 ***	-4.31	-0.300 **	-2.66	-0.076	-0.84	-1.468 ***	-3.53
Jianghuai	0.675 **	3.18	-0.581 *	-1.97	0.125	1.35	0.067	0.94	0.207	0.67
Sunan	0.815 ***	3.89	-0.597 +	-1.80	0.307 **	2.99	0.073	0.94	0.592	1.18
Whole	0.526 **	2.70	-0.701 **	-2.92	0.046	0.61	0.014	0.12	-0.245	-0.74

Note: +, *, ** and *** indicate the significance level of 0.1, 0.05, 0.01, and 0.001, respectively. β is the estimated slope of ET_{ref} trends, $\beta > 0$ and $\beta < 0$ indicate an increasing and a decreasing trend, respectively.

ET_{ref} showed a significant increasing tendency in spring and decreasing tendency in the summer, with rates of $0.526 \text{ mm}\cdot\text{a}^{-2}$ and $-0.701 \text{ mm}\cdot\text{a}^{-2}$, respectively, at the seasonal scale. The trend of ET_{ref} in winter was lower than in autumn. ET_{ref} in spring showed an increasing trend, especially significant in the Jianghuai and Sunan regions. The most significant decreasing trend of ET_{ref} was presented in the summer, particularly in Huaibei. A slight increasing trend was shown in the whole region in autumn, mainly due to the slight significant declining trend in Huaibei region combined with the slight significant increasing trends in Jianghuai and Sunan regions. Despite a decreasing trend shown in winter for the Huaibei region, the whole region exhibited a slight increasing trend, mainly due to the contributions of the slight increasing trends in the Jianghuai and Sunan regions.

The slopes of linear trends in climatic factors are shown in Table 3. Mean temperature in different seasons and regions revealed a significant increasing tendency, except for the summer season. On the contrary, wind speed and sunshine duration were shown to have significant declining

trends, in addition to the sunshine duration in spring, which demonstrated a slight decreasing trend in the Huaibei region and a slight increasing trend in the Jianghuai and Sunan regions. However, compared to the other three climatic factors, the change trend of VP is too small, only exhibiting a significant downward trend in summer, except for the Huaibei region.

Table 3. Temporal trends for climatic factors in Jiangsu province from 1961 to 2015.

Variable	Season	Huaibei	Jianghuai	Sunan	Whole
TA ($^{\circ}C \cdot a^{-1}$)	Spring	0.0348 ***	0.0382 ***	0.0439 ***	0.0391 ***
	Summer	0.0053	0.0113	0.0151 *	0.0111
	Autumn	0.0221 ***	0.0261 ***	0.0336 ***	0.0267 ***
	Winter	0.0390 ***	0.0319 ***	0.0333 ***	0.0344 ***
	Annual	0.0242 ***	0.0267 ***	0.0310 ***	0.0274 ***
VP ($kPa \cdot a^{-1}$)	Spring	0.000858	-0.000089	-0.000865	0.000022
	Summer	-0.000753	-0.001831 *	-0.002048 **	-0.001572 *
	Autumn	0.000762	0.000396	-0.000248	0.000382
	Winter	0.000667	0.000682	0.000658	0.000644
	Annual	0.000512	-0.000223	-0.000563	-0.000007
WS ($m \cdot s^{-1} \cdot a^{-1}$)	Spring	-0.0398 ***	-0.0293 ***	-0.0307 ***	-0.0332 ***
	Summer	-0.0297 ***	-0.0194 ***	-0.0217 ***	-0.0230 ***
	Autumn	-0.0301 ***	-0.0228 ***	-0.0244 ***	-0.0251 ***
	Winter	-0.0334 ***	-0.0281 ***	-0.0310 ***	-0.0305 ***
	Annual	-0.0341 ***	-0.0250 ***	-0.0268 ***	-0.0279 ***
SD ($h \cdot a^{-1}$)	Spring	-0.0042	0.0079	0.0071	0.0049
	Summer	-0.0442 ***	-0.0392 ***	-0.0417 ***	-0.0420 ***
	Autumn	-0.0207 **	-0.0092	-0.0104 +	-0.0121 *
	Winter	-0.0238 ***	-0.0170 **	-0.0151 **	-0.0190 **
	Annual	-0.0239 ***	-0.0152 ***	-0.0169 ***	-0.0179 ***

Note: +, *, ** and *** indicate the significance level of 0.1, 0.05, 0.01, and 0.001, respectively.

3.3. Sensitivity Coefficients of ET_{ref} to Climatic Factors

The sensitivity coefficients of seasonal and annual trends of ET_{ref} to each climatic factor by partial derivative are displayed in Figure 3. There are clear differences in the sensitivity characteristics for the four climatic factors and a slight discrepancy exists in the three regions of Jiangsu province. Generally, TA (air temperature), WS (wind speed), and SD (sunshine duration) produced a positive effect, whereas the VP (actual vapor pressure) had an adverse effect on seasonal and annual ET_{ref} . The results show that $S(TA)$ and $S(SD)$ were larger in the summer, but smaller in the winter, indicating that ET_{ref} was most sensitive to TA and SD in the summer compared to other seasons. The sensitivity coefficient of ET_{ref} to climatic factors ranked in a sequence as $VP > TA > SD > WS$. It can be said that the actual vapor pressure (VP) and air temperature (TA) were the greatest sensitive factors, while wind speed (WS) was shown to be the least sensitive factor of ET_{ref} , contrary to TA and SD , which had a relatively higher value in winter but lower in summer (Figure 3).

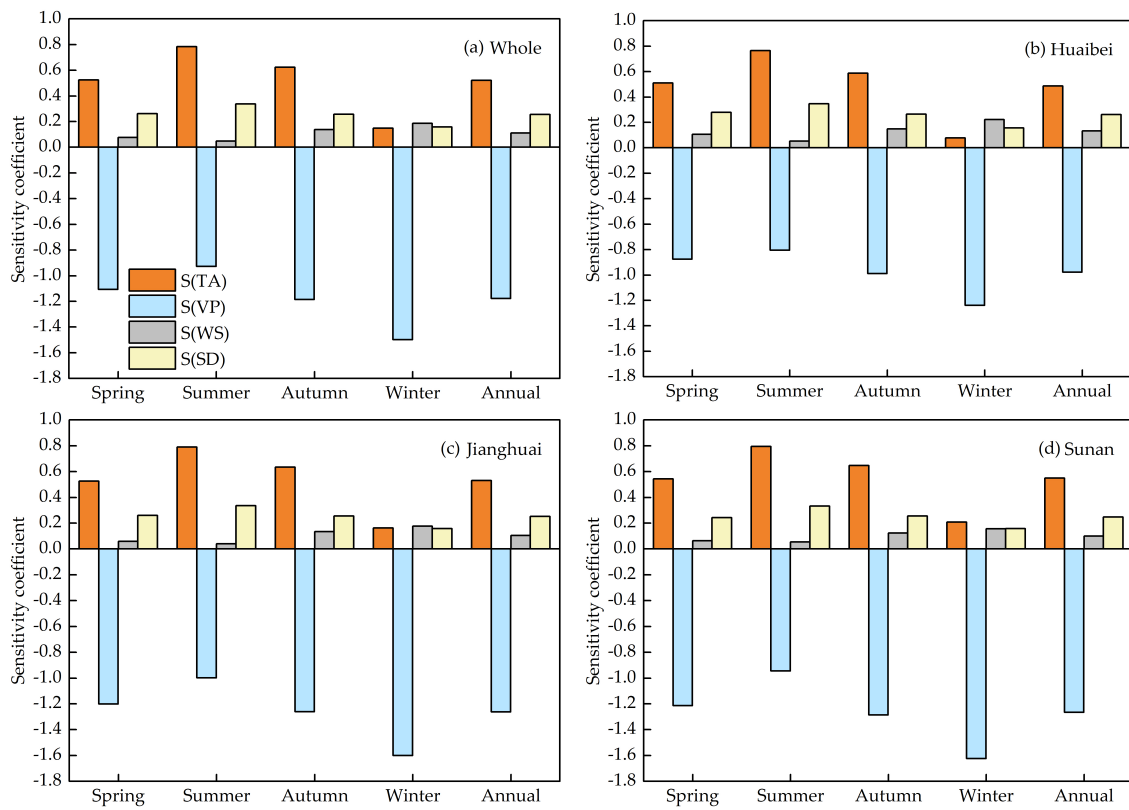


Figure 3. Sensitivities of seasonal and annual ET_{ref} in relation to climatic factors in (a) Whole, (b) Huaibei, (c) Jianghuai, and (d) Sunan regions of the Jiangsu province from 1961 to 2015.

3.4. Contributions of Climatic Factors to the Trends in ET_{ref}

The original and detrended climatic factors over the whole Jiangsu province are presented in Figure 4. Noticeable differences can be seen between the original and detrended datasets for each climatic factor, with a negative trend for TA and positive trends for VP, WS, and SD. The detrended TA was lower than the original data series, whereas the detrended VP, WS, and SD were higher than the original data series, especially the most obvious difference in WS. However, the difference between the original and detrended data series of VP was smaller than for the other three climatic factors at an annual scale in the whole region.

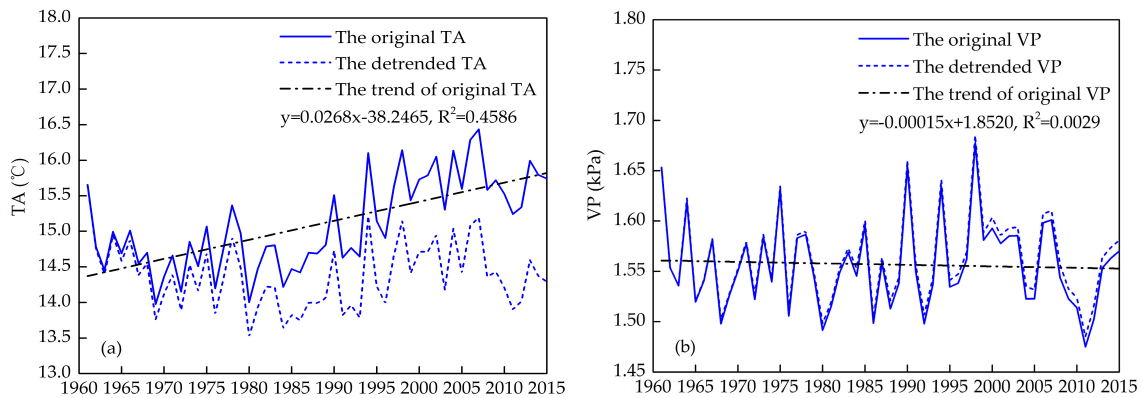


Figure 4. Cont.

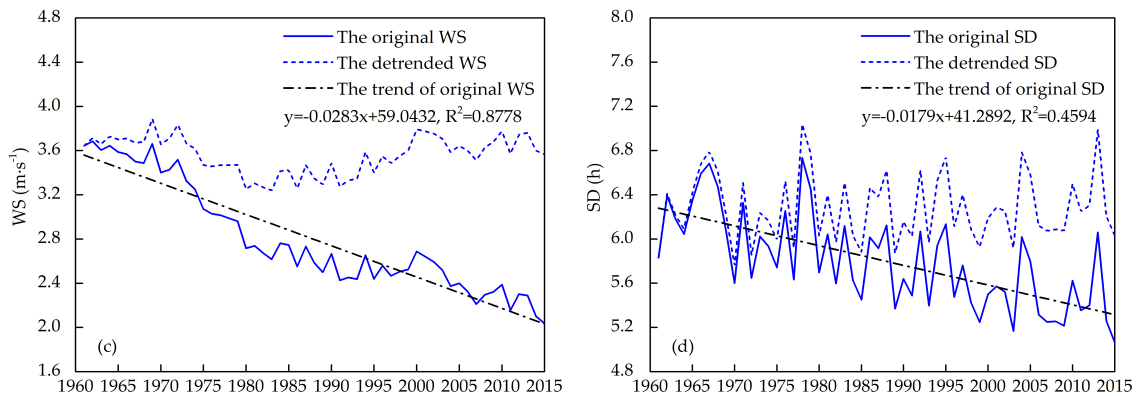


Figure 4. The original and detrended climatic factors (a) TA, (b) VP, (c) WS, and (d) SD for the whole of Jiangsu province during 1961–2015.

To understand a change event in seasonal and annual ET_{ref} due to the contributing factors, it is essential to analyze the contribution of each climatic factor to the change in seasonal and annual ET_{ref} . Results in Figure 5 demonstrate that the most important climatic factor dominating the trends in annual ET_{ref} on the whole Jiangsu province followed the order $WS > SD > TA > VP$. In general, the ET_{ref} recalculated with detrended TA and detrended VP was smaller than that calculated from the original climatic factors. On the contrary, the ET_{ref} recalculated with detrended WS and detrended SD was larger than that calculated from the original climatic factors. In other words, TA and VP had positive contributions to ET_{ref} , except VP in the Huaibei region, which exhibited a negative contribution, while WS and SD showed the opposite ones. In the end, the negative contributions would offset the positive one.

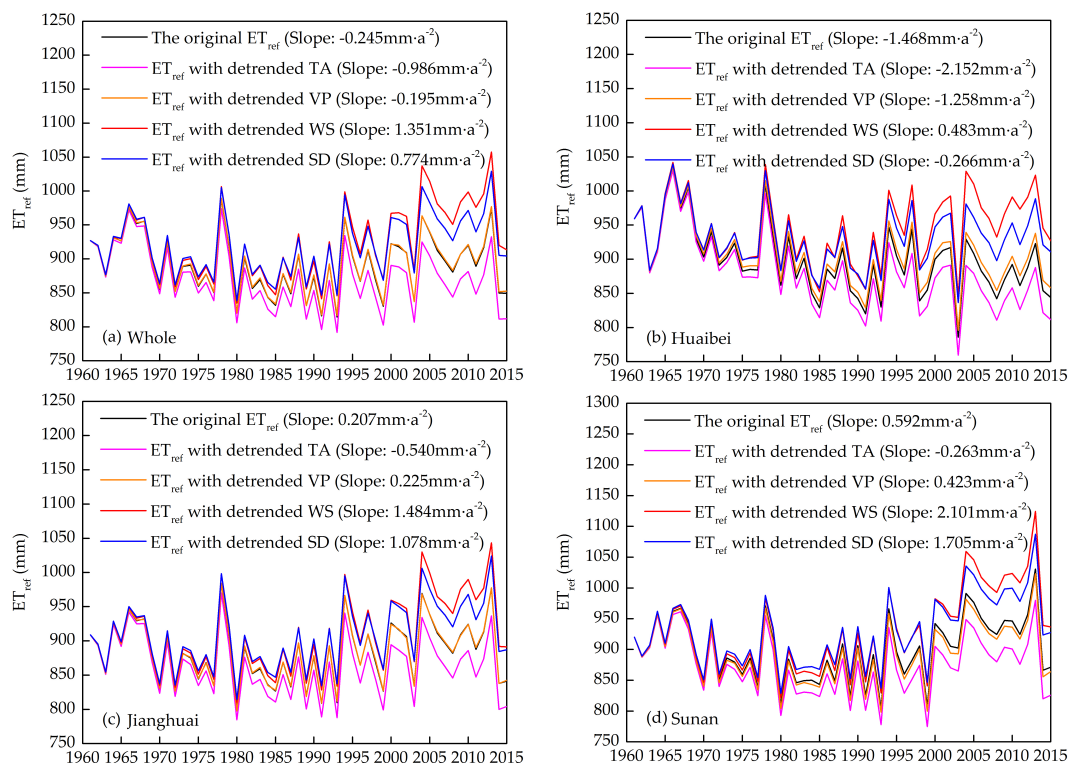


Figure 5. Contributions of climatic factors to the trends in ET_{ref} in (a) Whole, (b) Huaibei, (c) Jianghuai, and (d) Sunan regions of the Jiangsu province during 1961–2015.

On the annual scale, the contributions of *WS* and *SD* were greater than the total contributions of *TA* and *VP*, indicating a downward trend of ET_{ref} in the whole of Jiangsu province. Nevertheless, the variations of the climatic factors in three sub-regions caused different contributions to ET_{ref} . Similar results of ET_{ref} calculated with detrended *WS*, *SD*, and *TA* can be found in each sub-region of Jiangsu province; however, a small but interesting difference can be obtained between the original ET_{ref} and the recalculated ET_{ref} with detrended *VP* in the three sub-regions. The recalculated ET_{ref} with detrended *VP* was higher than that calculated from the original climatic factors in the Huaibei region; on the contrary, the result was opposite in the Sunan region, which exhibited a lower value compared with the original ET_{ref} . The reverse results demonstrated the varying trend of *VP* in the annual scale, which had been detected in Table 3; this also means it plays an important role in the contribution of an ET_{ref} trend across the different regions to some extent, although the variation is small and non-significant. From the results presented above, the contribution of ET_{ref} was a synergistic effect of various climatic factors; for example, significant decreasing *WS* and *SD* were the most crucial factors for the decreasing trend in ET_{ref} . *TA* was the main contributing factor to the increasing trend in ET_{ref} in each region of Jiangsu province, followed by *WS* and *SD*. The non-significant trend in *VP* made the smallest contribution to the trend of ET_{ref} ; however, it could not be ignored due to the variability and the effect of the contribution to ET_{ref} , as well as being the most sensitive factor to ET_{ref} . In contrast, the contribution of *WS* was greater than other factors.

On the seasonal scale, due to the limited space, we established an assessment index *R* that was used to quantify the contributions of *TA*, *VP*, *WS*, and *SD* to the change trends of ET_{ref} . Similar findings like Figure 5 can be obtained from Table 4, where *TA* had a positive contribution to the trend of ET_{ref} ; however, *WS* and *SD* had an adverse contribution in most regions except Jianghuai and Sunan in spring. In spring, the contribution of *TA* was the largest, followed by *WS* and *SD* except for the Huaibei region, whereas *WS* made a much greater contribution, followed by *TA*, *VP*, and *SD*. In summer, the contribution of *SD* played a dominant role in each region. In autumn, the contribution of *WS* was larger than other climatic factors, followed by *TA*, *SD*, and *VP*. Meanwhile, in winter, the contribution of the *WS* to ET_{ref} was much stronger than in the other three seasons. *TA* was the unique positive contributing factor, followed by *WS*, which led to an increasing trend in ET_{ref} . However, contrary to our expectations, the contribution of *VP* was much greater than in other seasons, and it also exhibited a negative contribution to ET_{ref} . This also confirmed the importance of *VP*, which has been discussed above, especially in the winter for the whole region.

Table 4. Values of assessment index *R* for quantifying the contributions of climatic factors to the change trends of seasonal ET_{ref} in each region of Jiangsu province.

Region	Spring				Summer				Autumn				Winter			
	<i>TA</i>	<i>VP</i>	<i>WS</i>	<i>SD</i>	<i>TA</i>	<i>VP</i>	<i>WS</i>	<i>SD</i>	<i>TA</i>	<i>VP</i>	<i>WS</i>	<i>SD</i>	<i>TA</i>	<i>VP</i>	<i>WS</i>	<i>SD</i>
Huaibei	1.69	-0.70	-2.97	-0.37	0.14	0.23	-1.53	-4.10	1.17	-0.62	-3.46	-1.28	2.99	-2.39	-5.59	-0.64
Jianghuai	1.97	0.04	-1.56	0.53	0.36	0.74	-0.81	-3.69	1.29	-0.37	-2.11	-0.36	2.51	-2.25	-3.26	-0.58
Sunan	2.21	0.74	-1.73	0.51	0.59	0.85	-1.12	-4.09	1.64	0.10	-2.23	-0.66	2.52	-2.16	-3.46	-0.75
Whole	1.95	-0.02	-2.05	0.24	0.35	0.62	-1.11	-3.91	1.34	-0.32	-2.52	-0.70	2.65	-2.27	-3.98	-0.64

Note: Values in bold face indicate the dominant contributing factors.

3.5. Evaporation Paradox Analysis with Trends of *TA* and ET_{ref}

The evaporation paradox has become a debatable issue against the backdrop of global climate warming and decreasing evaporation scenarios [23]. It can be seen from Figure 6 that the mean temperature (1961–2015) had a significant increase in the whole of Jiangsu province when the rate of climatic tendency ranged between $0.013\text{ }^{\circ}\text{C}\cdot\text{a}^{-1}$ and $0.047\text{ }^{\circ}\text{C}\cdot\text{a}^{-1}$, with an especially high rate in the Jianghuai and Sunan regions. The climatic trend rate of ET_{ref} ranged between $-2.46\text{ mm}\cdot\text{a}^{-2}$ and $2.93\text{ mm}\cdot\text{a}^{-2}$, indicating a distinctly various distribution on the spatial scale. A positive trend of ET_{ref} was found in the Jianghuai and Sunan regions, while a significant overall downward trend was observed in Huaibei; the reason is the decrease of *WS* and *SD*, despite being accompanied by a significant increase in *TA*.

Meanwhile, in the spring, the distribution of the TA was the same as the annual—both strong increasing tendencies. ET_{ref} increased significantly in Jianghuai and Sunan and had increasing and decreasing trends, both insignificant, in Huaibei. In summer, a significant increasing trend of TA showed in southeast Jiangsu province; moreover, the increasing trend in other regions was insignificant. ET_{ref} showed a downward trend, especially significant in Huaibei and along the lower Yangtze River Basin. In autumn, both the TA and ET_{ref} were similar to the annual scale distribution. In the winter, a significant downward trend of ET_{ref} existed only in Huaibei, although a strong upward trend of TA was exhibited in the whole of Jiangsu province. These results indicated that the evaporation paradox was apparent in Jiangsu province, especially in summer and in the Huaibei region in autumn, and also on an annual scale.

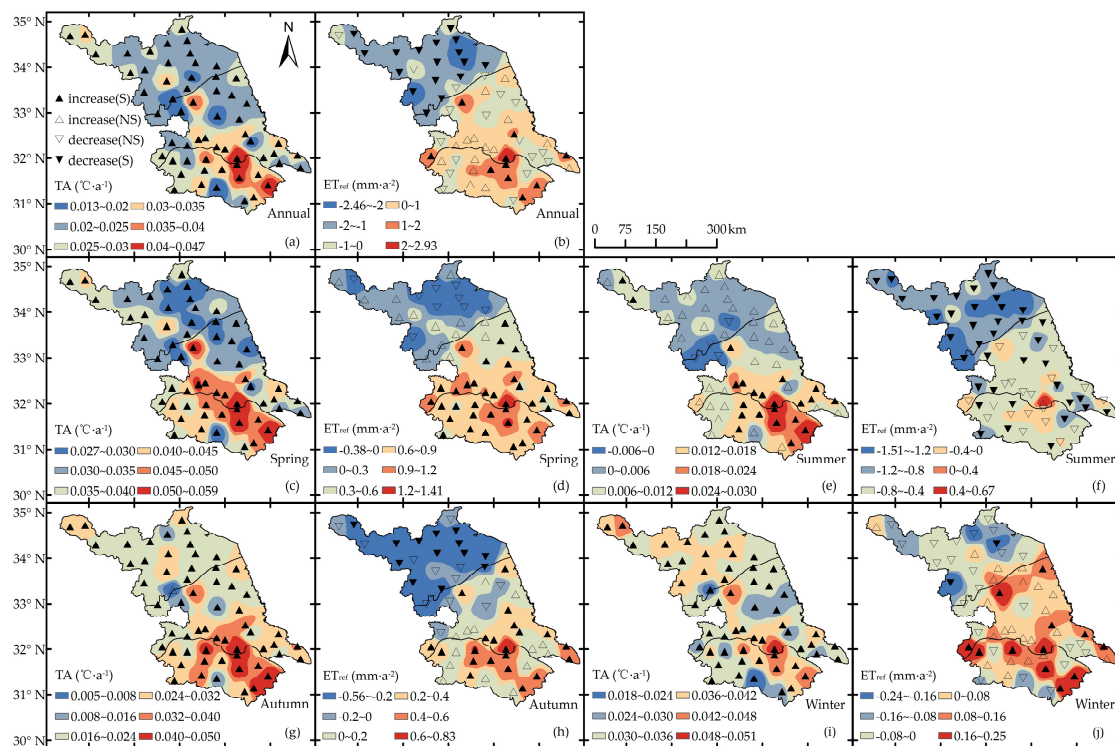


Figure 6. Spatial distributions of climate tendency rates of the TA and ET_{ref} from 1961 to 2015 in Jiangsu province. **Note:** S and NS represent significant and non-significant trends at the 0.05 level of the TA and ET_{ref} , respectively. (a), (c), (e), (g), and (i) represent the trends of TA in annual, spring, summer, autumn, and winter seasons, respectively, (b), (d), (f), (h), and (j) represent the trends of ET_{ref} in annual, spring, summer, autumn and winter seasons, respectively.

4. Discussions

4.1. Change Trend of ET_{ref} and Its Contributing Factors

This study is driven by the need to know why ET_{ref} has changed in Jiangsu province and what factors are responsible. This study, therefore, applied physical modeling to determine the sensitivity of ET_{ref} to different climatic factors and a detrending method to identify the main contributions of climatic factors to ET_{ref} changes. In the current research, decreasing and increasing trends were found in Jiangsu province. A decreasing trend showed in annual and summer ET_{ref} , while an increasing trend was observed in spring, autumn, and winter ET_{ref} for the whole province.

The results in this study highlighted the greater sensitivity of ET_{ref} in Jiangsu province to TA , followed by SD during the summer, when ET_{ref} reached its peak position. VP had a much higher impact on ET_{ref} than the other three climatic factors, especially in the winter, when ET_{ref} reached its

lowest. WS had the smallest influence on the ET_{ref} estimation, with a higher sensitivity in the winter but lower in the summer. The sensitivity of seasonal and annual ET_{ref} to climatic factors was variable in different regions. Furthermore, the declining ET_{ref} trend was more sensitive to VP in the present study. Our findings provide a new perspective for further study, due to the fact that previous research usually chose relative humidity as the influence factor, such as in the basins of the Yangtze River, Tao'er River, and Wei River in China [4,8,51–53]. However, the variation of ET_{ref} was most sensitive to WS in the basins of the Shiyang River and Jinghe River [11,54]. In addition, TA and R_n were the utmost sensitive parameters in the Haihe River basin and Poyang Lake catchment in China [55,56]. It can be said that ET_{ref} has various responses to meteorological factors in various regions of China.

The contributions of climatic factors to the changes in ET_{ref} were also diverse in various regions. In this study, WS was the primary variable, followed by SD to annual ET_{ref} across the whole of Jiangsu province, which was similar to the outcomes reported by Wang et al. [36] in the Yellow River basin. Zhang et al. [57] indicated that the decreasing trend in ET_{ref} was due to a decrease in WS and R_n across the Tibetan Plateau. However, WS and TA were the predominant factors contributing to its inter-annual variation in Northwest China [58]. Results of changes in ET_{ref} and its contributing factors in Jiangsu province agreed with the conclusion of Gao et al. [59], who showed that WS was the chief factor, followed by R_n in the west of the Liao River basin. In addition, we found that VP is also an important influence factor, especially in winter in the whole region, although the change trend of VP is very small.

As the decreasing WS had been widely reported in various regions, Zhang et al. [60] proposed that the weakening atmospheric circulation may be the explanation for the WS decreasing. However, the significant weakened East Asian Monsoon is also closely linked to decreasing WS [26,61]. In addition, the increase of terrestrial surface roughness due to the increased vegetation coverage, such as the afforestation put forward by Vautard et al. [62], could also explain the decreasing WS . Meanwhile, the significantly decreasing SD also made a negative contribution to the decreasing ET_{ref} , closely followed by WS , especially in the summer, while the functional mechanism of the decreasing SD is still a matter for debate. A significant number of studies have shown that decreasing solar radiation had occurred in different regions before 1980s [63,64]; however, this decreasing trend has been mitigated since the 1990s, via the phenomenon we call “From dimming to Brightening” [65–67]. Combined with the sunshine duration in Figure 4, this phenomenon is seemingly not evident in Jiangsu province. Meanwhile, some recent studies have shown that the decreasing SD is mainly caused by the increased regional cloud cover [65,68] and increasing aerosol loading from anthropogenic emissions of pollutants [69,70], coupled with significant declining WS . These phenomena were confirmed by Zhang et al. [71] in east and south China. Furthermore, due to the absence of measured solar radiation, the parameters (a and b) in the Angstrom formula might vary across the past 55 years as the aerosol optical depths have changed in this region. This is an important potential constraint on the observed effects of changes in R_n on ET_{ref} , which will surely have been underestimated as a result of using this approximation of R_s from the sunshine duration.

4.2. Evaporation Paradox

The “evaporation paradox” is a controversial topic that has earned attention among researchers worldwide [22,72]. The results indicated that the evaporation paradox was apparent in Jiangsu province, mainly in the summer and in Huaibei region in the autumn. Furthermore, the significant increase in TA in Jiangsu province appeared to be in agreement with the global warming reported in recent decades [10]. However, interestingly, TA showed a significant result with the decrease of ET_{ref} (Tables 2 and 3). These findings disagree with the earlier results of Ye et al. [56], Liu and Zeng [73], and Li et al. [74]. The “evaporation paradox” occurred due to the significant decrease of WS and SD in the whole of Jiangsu province. The strong influences on ET_{ref} from these contributing factors compensate for the decrease of ET_{ref} from the significant increase in TA , resulting in an overall decrease in ET_{ref} . Such findings are echoed by the similar works of Roderick and Farquhar [17,18], Xu et al. [8],

Cong et al. [14], and Zuo et al. [52]. However, it is evident that ET_{ref} has decreased in many parts of the world in the context of global warming. Xu et al. [75] summarized the major reason: higher air temperature leads to more powerful atmospheric water holding capacity, resulting in an increase of cloud cover and a decline of solar radiation reaching the Earth's surface.

4.3. Influence on Agricultural Production and Water Management

Jiangsu is a major agricultural province in China, and main crops such as winter wheat and single-season rice have been greatly affected by climate change, especially in regions with variable climate [38]. Decreasing wind speed (WS), sunshine duration (SD), actual vapor pressure (VP), and increasing air temperature (TA) were the driving forces behind a slightly decreasing ET_{ref} in the Jiangsu province, and climate change may complicate impacts on agricultural production and water resource management. The significantly decreasing ET_{ref} in summer may be responsible for greater water reserves and an increase in regional vegetation cover and crop production, especially the cultivation of single-season rice across the whole of Jiangsu province, which further assists with irrigation water resource distribution and management. Meanwhile, excessive rainfall caused frequent floods in summer; this should be paid more attention, especially in the Huaibei region, which belongs to the Huai River Basin [76]. However, the increasing ET_{ref} in autumn would not be suitable for the seeding of winter wheat in Jianghuai and Sunan, and could affect crop growth and development. Moreover, the slight increase in ET_{ref} in the winter would reduce the soil moisture and be harmful for the overwintering of winter wheat. More seriously, the significant increase in ET_{ref} in spring may inhibit the reviving and jointing of winter wheat and would likely increase the frequency of spring droughts, despite the abundant rainfall in this province of eastern China. However, the significant decrease in ET_{ref} in Huaibei region in summer, autumn, and on an annual scale would promote single-season rice and winter wheat growth, whereas the slight decreasing trend of ET_{ref} in the winter and the increasing trend in the spring could not be ignored.

For the past few years, with the rapid increase of population and intensified land utilization, the rising problems of regional water resources and ecological environment have been increasingly highlighted. These issues deserve more attention in future studies on how the changes of annual and seasonal ET_{ref} are associated with potential and actual evapotranspiration. Integration with remote sensing techniques will be important to determine the subsequent effect on the regional water balance of Jiangsu province in the light of population growth, urbanization, and climate change.

5. Conclusions

This research examined the spatiotemporal changes in reference evapotranspiration (ET_{ref}) based on the Penman–Monteith FAO 56 model in Jiangsu province, a major economic and agricultural province of eastern China, by studying the daily weather data of 60 meteorological stations from 1961 to 2015. In addition, physical and mathematical modeling and the detrending method were applied to determine the sensitivity of ET_{ref} and the main contributing climatic factors to ET_{ref} . The following findings were drawn from this study:

- (1) Decreasing and increasing trends were identified in Jiangsu province at seasonal and annual scales. A significant declining trend of ET_{ref} was observed in the Huaibei region, while other regions demonstrated a slight rising trend of ET_{ref} . ET_{ref} also showed a significant increasing tendency in spring and a decreasing tendency in summer.
- (2) VP was the most sensitive climatic factor, followed by TA , SD , and WS in each region. ET_{ref} was more sensitive to TA and SD in the summer but less so in the winter; however, the sensitivities of WS and VP to ET_{ref} were the opposite in Jiangsu province.
- (3) The contribution of ET_{ref} was a synergistic effect of various climatic factors; significantly decreasing WS and SD were the most crucial factors contributing to the decreasing trend in ET_{ref} , while TA was the main contributing factor for the increasing trend in ET_{ref} , followed by

WS and SD. The non-significant trend in VP made the smallest contribution to the trend of ET_{ref} ; however, it could not be ignored due to the variability and the effect of the contribution to ET_{ref} , as well as being the most sensitive factor to ET_{ref} , especially in winter.

- (4) It was evident that the phenomenon of evaporation paradox was apparent in Jiangsu province, especially in the summer and in the Huaibei region in the autumn.
- (5) In summary, these results will provide a theoretical background and practical guidance for future water resource distribution and management and lay the basis for the future study of agricultural water requirements and economic development in the whole of Jiangsu province in the scenario of climate change.

Acknowledgments: Thanks to the editors and two anonymous reviewers for all the constructive comments and useful suggestions that helped us to upgrade the quality of this paper substantially. We also acknowledge the financial support from the China Special Fund for Meteorological Research in the Public Interest (GYHY201506001) and the National Natural Science Foundation of China (Grant No. 41405111).

Author Contributions: Shuanghe Shen supervised the research. Ronghao Chu and Meng Li analyzed the data, conceived, designed, and performed the research. Abu Reza Md. Towfiqul Islam modified and polished the English in this paper. Wen Cao proposed some constructive suggestions about the methods. Sulin Tao and Ping Gao provided the meteorological data.

Conflicts of Interest: The authors declare no conflict of interest.

Appendix A

The specific derived expressions for sensitivity coefficients:

We divided Equation (1) into two parts as follows: the radiative (ET_{rad}) and aerodynamic (ET_{aero}) components:

$$ET_{ref} = ET_{rad} + ET_{aero} = \frac{0.408\Delta(R_n - G)}{\Delta + \gamma(1 + 0.34u_2)} + \frac{\gamma \frac{900}{T+273} u_2 (e_s - e_a)}{\Delta + \gamma(1 + 0.34u_2)}$$

$$e_s = 0.6108 \exp\left(\frac{17.27T}{T + 237.3}\right)$$

$$\Delta = \frac{4098 \times \left[0.6108 \exp\left(\frac{17.27T}{T+237.3}\right)\right]}{(T + 237.3)^2} = \frac{4098 \times e_s}{(T + 237.3)^2}$$

$$P = 101.3 \left(\frac{273 + T - 0.0065h}{273 + T}\right)^{5.26},$$

where P is atmospheric pressure (kPa) and h is the elevation above sea level.

$$\gamma = \frac{0.00163P}{\lambda},$$

where λ is the latent heat of vaporization, 2.45 (MJ·kg⁻¹).

TA (Air mean temperature):

$$\frac{\partial e_s}{\partial T} = e_s \left(-17.27 \times 237.3 \times (-1) \times (237.3 + T)^{-2}\right)$$

$$\frac{\partial \Delta}{\partial T} = \frac{4098 \frac{\partial e_s}{\partial T}}{(237.3 + T)^2} + \frac{4098 \times e_s \times (-2)}{(237.3 + T)^3}$$

$$\frac{\partial P}{\partial T} = 101.3 \times 5.26 \times \left(1 - \frac{0.0065 \times h}{273 + T}\right)^{4.26} \times \frac{0.0065 \times h}{(273 + T)^2}$$

$$\frac{\partial \gamma}{\partial T} = \frac{0.00163 \times \frac{\partial P}{\partial T}}{\lambda} + \frac{0.00163 \times P \times 0.002361}{\lambda^2}$$

$$\frac{\partial R_n}{\partial T} = 4.903 \times 10^{-9} \left(\frac{(T_{\max}+273)^4 + (T_{\min}+273)^4}{2} \right) \times \left(-0.14 \times 0.5 \times (e_s \times RH)^{-0.5} \times RH \times \frac{\partial e_s}{\partial T} \right) \\ \times \left(1.35 \times \frac{R_s}{R_{so}} - 0.35 \right)$$

$$ET_{rad} = 0.408(R_n - G) \times \frac{\Delta}{\Delta + \gamma(1 + 0.34u_2)} = ET_{rad_A} \times ET_{rad_B}$$

$$\frac{\partial ET_{rad}}{\partial ET_{rad_A}} = \frac{-1 \times \frac{\partial R_n}{\partial T} \times 0.408 \times \Delta}{\Delta + \gamma(1 + 0.34u_2)}$$

$$\frac{\partial ET_{rad}}{\partial ET_{rad_B}} = 0.408 \times R_n \times \left[\frac{\frac{\partial \Delta}{\partial T}}{\Delta + \gamma(1 + 0.34u_2)} - \frac{\Delta \times \left(\frac{\partial \Delta}{\partial T} + \frac{\partial \gamma}{\partial T} \times (1 + 0.34u_2) \right)}{(\Delta + \gamma(1 + 0.34u_2))^2} \right]$$

$$\frac{\partial ET_{rad}}{\partial T} = \frac{\partial ET_{rad}}{\partial ET_{rad_A}} + \frac{\partial ET_{rad}}{\partial ET_{rad_B}}$$

$$ET_{aero} = \left[\frac{900\gamma}{\Delta + \gamma(1 + 0.34u_2)} \right] \times [u_2 \times e_s \times (1 - RH)] \times \left[\frac{1}{273 + T} \right] = ET_{aero_A} \times ET_{aero_B} \times ET_{aero_C}$$

$$\frac{\partial ET_{aero}}{\partial ET_{aero_A}} = \left[900 \times \left(\frac{\frac{\partial \gamma}{\partial T}}{(\Delta + \gamma(1 + 0.34u_2))} - \frac{\gamma \left(\frac{\partial \Delta}{\partial T} + \frac{\partial \gamma}{\partial T} (1 + 0.34u_2) \right)}{(\Delta + \gamma(1 + 0.34u_2))^2} \right) \right] \times ET_{aero_B} \times ET_{aero_C}$$

$$\frac{\partial ET_{aero}}{\partial ET_{aero_B}} = \left[u_2 \times (1 - RH) \times \frac{\partial e_s}{\partial T} \right] \times ET_{aero_A} \times ET_{aero_C}$$

$$\frac{\partial ET_{aero}}{\partial ET_{aero_C}} = \left[\frac{-1}{(273 + T)^2} \right] \times ET_{aero_A} \times ET_{aero_B}$$

$$\frac{\partial ET_{aero}}{\partial T} = \frac{\partial ET_{aero}}{\partial ET_{aero_A}} + \frac{\partial ET_{aero}}{\partial ET_{aero_B}} + \frac{\partial ET_{aero}}{\partial ET_{aero_C}}$$

$$\frac{\partial ET_{ref}}{\partial T} = \frac{\partial ET_{rad}}{\partial T} + \frac{\partial ET_{aero}}{\partial T}$$

VP (Actual vapor pressure):

$$\frac{\partial ET_{rad}}{\partial VP} = -4.903 \times 10^{-9} \times \left[\frac{(T_{\max}+273)^4 + (T_{\min}+273)^4}{2} \right] \times (-0.14) \times 0.5 \times e_a^{-0.5} \\ \times \left(1.35 \frac{R_s}{R_{so}} - 0.35 \right) \times \frac{0.408\Delta}{\Delta + \gamma(1 + 0.34u_2)}$$

$$\frac{\partial ET_{aero}}{\partial VP} = \frac{-\gamma \frac{900}{273 + T} \times u_2}{\Delta + \gamma(1 + 0.34u_2)}$$

$$\frac{\partial ET_{ref}}{\partial VP} = \frac{\partial ET_{rad}}{\partial VP} + \frac{\partial ET_{aero}}{\partial VP}$$

WS (Wind speed):

$$\frac{\partial ET_{rad}}{\partial WS} = (0.408 \times \Delta \times R_n) \times (-1) \times (\Delta + \gamma(1 + 0.34u_2))^{-2} \times \gamma \times 0.34$$

$$ET_{aero} = u_2 \times \left[\frac{\gamma \frac{900}{T+273} (e_s - e_a)}{\Delta + \gamma(1 + 0.34u_2)} \right] = ET_{aero_A} \times ET_{aero_B}$$

$$\frac{\partial ET_{aero}}{\partial ET_{aero_A}} = \frac{\gamma \frac{900}{T+273} (e_s - e_a)}{\Delta + \gamma(1 + 0.34u_2)}$$

$$\frac{\partial ET_{aero}}{\partial ET_{aero_B}} = \left[\frac{\gamma \times 900}{273 + T} \times u_2 \times e_s \times (1 - RH) \right] \times (-1) \times [\Delta + \gamma(1 + 0.34u_2)]^{-2} \times \gamma \times 0.34$$

$$\frac{\partial ET_{aero}}{\partial WS} = \frac{\partial ET_{aero}}{\partial ET_{aero_A}} + \frac{\partial ET_{aero}}{\partial ET_{aero_B}}$$

$$\frac{\partial ET_{ref}}{\partial WS} = \frac{\partial ET_{rad}}{\partial WS} + \frac{\partial ET_{aero}}{\partial WS}$$

SD (Sunshine duration):

$$\frac{\partial R_n}{\partial R_s} = (1 - 0.23) - 4.093 \times 10^{-9} \times \left[\frac{(T_{max}+273)^4 + (T_{min}+273)^4}{2} \right] \times (0.34 - 0.14 \times \sqrt{e_a}) \times 1.35 \times \frac{R_s}{R_{so}^2}$$

$$\frac{\partial ET_{ref}}{\partial R_s} = \frac{\partial ET_{rad}}{\partial R_s} = \frac{\partial R_n}{\partial R_s} \times \frac{0.408\Delta}{\Delta + \gamma(1 + 0.34u_2)}$$

$$\frac{\partial ET_{ref}}{\partial SD} = \frac{\partial ET_{rad}}{\partial SD} = \frac{\partial ET_{rad}}{\partial R_s} \times 0.5 \times \frac{R_a}{N}$$

References

- Jhahharia, D.; Shrivastava, S.K.; Sarkar, D.; Sarkar, S. Temporal characteristics of pan evaporation trends under the humid conditions of northeast India. *Agric. For. Meteorol.* **2009**, *149*, 763–770. [CrossRef]
- Sentelhas, P.C.; Gillespie, T.J.; Santos, E.A. Evaluation of FAO Penman—Monteith and alternative methods for estimating reference evapotranspiration with missing data in Southern Ontario, Canada. *Agric. Water Manag.* **2010**, *97*, 635–644. [CrossRef]
- Burn, D.H.; Hesch, N.M. Trends in evaporation for the Canadian Prairies. *J. Hydrol.* **2007**, *336*, 61–73. [CrossRef]
- Shan, N.; Shi, Z.; Yang, X.; Gao, J.; Cai, D. Spatiotemporal trends of reference evapotranspiration and its driving factors in the Beijing-Tianjin Sand Source Control Project Region, China. *Agric. For. Meteorol.* **2015**, *200*, 322–333. [CrossRef]
- Tabari, H.; Aeini, A.; Talaee, P.H.; Some'e, B. Spatial distribution and temporal variation of reference evapotranspiration in arid and semi-arid regions of Iran. *Hydrol. Process.* **2012**, *26*, 500–512. [CrossRef]
- Zhang, C.; Shen, Y.; Liu, F.; Meng, L. Changes in reference evapotranspiration over an agricultural region in the Qinghai-Tibetan plateau, China. *Theor. Appl. Climatol.* **2016**, *123*, 107–115. [CrossRef]
- Gao, X.; Peng, S.; Wang, W.; Xu, J.; Yang, S. Spatial and temporal distribution characteristics of reference evapotranspiration trends in Karst area: A case study in Guizhou Province, China. *Meteorol. Atmos. Phys.* **2016**, *128*, 677–688. [CrossRef]
- Xu, C.; Gong, L.; Jiang, T.; Chen, D.; Singh, V.P. Analysis of spatial distribution and temporal trend of reference evapotranspiration and pan evaporation in Changjiang (Yangtze River) catchment. *J. Hydrol.* **2006**, *327*, 81–93. [CrossRef]
- Srivastava, P.; Han, D.; Ramirez, M.; Islam, T. Comparative assessment of evapotranspiration derived from NCEP and ECMWF global datasets through Weather Research and Forecasting model. *Atmos. Sci. Lett.* **2013**, *14*, 118–125. [CrossRef]
- Solomon, S.; Qin, D.; Manning, M.; Chen, Z.; Marquis, M.; Averyt, K.; Miller, H. *Contribution of Working Group I to the Fourth Assessment Report of the Intergovernmental Panel on Climate Change*; Cambridge University Press: Cambridge, UK, 2007.
- Xu, L.; Shi, Z.; Wang, Y.; Zhang, S.; Chu, X.; Yu, P.; Xiong, W.; Zuo, H.; Wang, Y. Spatiotemporal variation and driving forces of reference evapotranspiration in Jing River Basin, northwest China. *Hydrol. Process.* **2015**, *29*, 4846–4862. [CrossRef]
- Xie, H.; Zhu, X.; Yuan, D. Pan evaporation modelling and changing attribution analysis on the Tibetan Plateau (1970–2012). *Hydrol. Process.* **2015**, *25*, 2164–2177. [CrossRef]
- Liu, Q.; McVicar, T.R. Assessing climate change induced modification of Penman potential evaporation and runoff sensitivity in a large water-limited basin. *J. Hydrol.* **2012**, *464*, 352–362. [CrossRef]

14. Cong, Z.T.; Yang, D.W.; Ni, G.H. Does evaporation paradox exist in China? *Hydrol. Earth Syst. Sci.* **2009**, *13*, 357–366. [[CrossRef](#)]
15. Liu, T.; Li, L.; Lai, J.; Liu, C.; Zhuang, W. Reference evapotranspiration change and its sensitivity to climate variables in southwest China. *Theor. Appl. Climatol.* **2016**, *125*, 499–508. [[CrossRef](#)]
16. Yang, H.; Yang, D. Climatic factors influencing changing pan evaporation across China from 1961 to 2001. *J. Hydrol.* **2012**, *414*, 184–193. [[CrossRef](#)]
17. Roderick, M.L.; Farquhar, G.D. Changes in Australian pan evaporation from 1970 to 2002. *Int. J. Climatol.* **2004**, *24*, 1077–1090. [[CrossRef](#)]
18. Roderick, M.L.; Farquhar, G.D. Changes in New Zealand pan evaporation since the 1970s. *Int. J. Climatol.* **2005**, *25*, 2031–2039. [[CrossRef](#)]
19. Chattopadhyay, N.; Hulme, M. Evaporation and potential evapotranspiration in India under conditions of recent and future climate change. *Agric. For. Meteorol.* **1997**, *87*, 55–73. [[CrossRef](#)]
20. Limjirakan, S.; Limsakul, A. Trends in Thailand pan evaporation from 1970 to 2007. *Atmos. Res.* **2012**, *108*, 122–127. [[CrossRef](#)]
21. Breña-Naranjo, J.A.; Laverde, M.A.; Pedrozo-Acuña, A. Changes in pan evaporation in Mexico from 1961 to 2010. *Int. J. Climatol.* **2016**, *23*, 361–387. [[CrossRef](#)]
22. Brutsaert, W.; Parlange, M. Hydrologic cycle explains the evaporation paradox. *Nature* **1998**, *396*, 30–30. [[CrossRef](#)]
23. Wang, J.; Wang, Q.; Zhao, Y.; Li, H.; Zhai, J.; Shang, Y. Temporal and spatial characteristics of pan evaporation trends and their attribution to meteorological drivers in the Three-River Source Region, China. *J. Geophys. Res. Atmos.* **2015**, *120*, 6391–6408. [[CrossRef](#)]
24. Hobbins, M.T.; Ramírez, J.A.; Brown, T.C. Trends in pan evaporation and actual evapotranspiration across the conterminous US: Paradoxical or complementary? *Geophys. Res. Lett.* **2004**, *31*, 405–407. [[CrossRef](#)]
25. Rotstayn, L.; Roderick, M.; Farquhar, G.D. A simple pan-evaporation model for analysis of climate simulations: Evaluation over Australia. *Geophys. Res. Lett.* **2006**, *33*, 254–269. [[CrossRef](#)]
26. Mcvicar, T.; Roderick, M.; Donohue, R.; Li, L.; Niel, T.G.V.; Thomas, A.; Grieser, J.; Jhajharia, D.; Himri, Y.; Mahowald, N.M.; et al. Global review and synthesis of trends in observed terrestrial near-surface wind speeds: Implications for evaporation. *J. Hydrol.* **2012**, *416–417*, 182–205. [[CrossRef](#)]
27. Allen, R.G.; Pereira, L.S.; Raes, D.; Smith, M. Crop evapotranspiration-Guidelines for computing crop water requirements-FAO Irrigation and drainage paper 56. *FAO Rome* **1998**, *300*, D05109.
28. Liu, X.; Zhang, D. Trend analysis of reference evapotranspiration in Northwest China: The roles of changing wind speed and surface air temperature. *Hydrol. Process.* **2013**, *27*, 3941–3948. [[CrossRef](#)]
29. McCuen, R.H. A sensitivity and error analysis of procedures used for estimating evaporation. *JAWRA J. Am. Water Resour. Assoc.* **1974**, *10*, 486–497. [[CrossRef](#)]
30. Li, Z.; Li, Z.; Xu, Z.; Zhou, X. Temporal variations of reference evapotranspiration in Heihe River basin of China. *Hydrol. Res.* **2013**, *44*, 904–916. [[CrossRef](#)]
31. Liu, Q.; Yang, Z.; Cui, B.; Sun, T. The temporal trends of reference evapotranspiration and its sensitivity to key meteorological variables in the Yellow River Basin, China. *Hydrol. Process.* **2010**, *24*, 2171–2181. [[CrossRef](#)]
32. Huo, Z.; Dai, X.; Feng, S.; Kang, S.; Huang, G. Effect of climate change on reference evapotranspiration and aridity index in arid region of China. *J. Hydrol.* **2013**, *492*, 24–34. [[CrossRef](#)]
33. Li, Z.; Feng, Q.; Liu, W.; Wang, T.; Gao, Y.; Wang, Y.; Cheng, A.; Li, J.; Liu, L. Spatial and temporal trend of potential evapotranspiration and related driving forces in Southwestern China, during 1961–2009. *Quat. Int.* **2014**, *336*, 127–144.
34. Liu, X.; Zhang, D.; Luo, Y.; Liu, C. Spatial and temporal changes in aridity index in northwest China: 1960 to 2010. *Theor. Appl. Climatol.* **2013**, *112*, 307–316. [[CrossRef](#)]
35. Wang, Y.; Jiang, T.; Bothe, O.; Fraedrich, K. Changes of pan evaporation and reference evapotranspiration in the Yangtze River basin. *Theor. Appl. Climatol.* **2007**, *90*, 13–23. [[CrossRef](#)]
36. Wang, W.; Shao, Q.; Peng, S.; Xing, W.; Yang, T.; Luo, Y.; Yong, B.; Xu, J. Reference evapotranspiration change and the causes across the Yellow River Basin during 1957–2008 and their spatial and seasonal differences. *Water Resour. Res.* **2012**, *48*. [[CrossRef](#)]

37. Shen, S.H.; Yang, S.B.; Zhao, Y.X.; Xu, Y.L.; Zhao, X.Y.; Wang, Z.Y.; Liu, J.; Zhang, W.W. Simulating the rice yield change in the middle and lower reaches of the Yangtze River under SRES B2 scenario. *Acta Ecol. Sin.* **2011**, *31*, 40–48. [[CrossRef](#)]
38. Tao, S.; Shen, S.; Li, Y.; Wang, Q.; Gao, P.; Mugume, I. Projected crop production under regional climate change using scenario data and modeling: Sensitivity to chosen sowing date and cultivar. *Sustainability* **2016**, *8*, 214. [[CrossRef](#)]
39. Pan, A.D.; Cao, Y.; Chen, H.S. Impacts of climate change on food-crops production in Jiangsu Province from 1986 to 2010. *Trans. Atmos. Sci.* **2013**, *36*, 217–228.
40. Peterson, T.C.; Easterling, D.R.; Karl, T.R.; Groisman, P.; Nicholls, N.; Plummer, N.; Torok, S.; Auer, I.; Boehm, R.; Gullett, D.; et al. Homogeneity adjustments of in situ atmospheric climate data: A review. *Int. J. Climatol.* **1998**, *18*, 1493–1517. [[CrossRef](#)]
41. Angstrom, A. Solar and terrestrial radiation. Report to the international commission for solar research on actinometric investigations of solar and atmospheric radiation. *Q. J. R. Meteorol. Soc.* **1924**, *50*, 121–126. [[CrossRef](#)]
42. Chen, R.; Kang, E.; Yang, J.; Lu, S.; Zhao, W. Validation of five global radiation models with measured daily data in China. *Energy Convers. Manag.* **2004**, *45*, 1759–1769. [[CrossRef](#)]
43. Mann, H.B. Nonparametric test against trend. *Econometrica* **1945**, *13*, 245–259. [[CrossRef](#)]
44. Kendall, M.G. A new measure of rank correlation. *Biometrika* **1938**, *30*, 81–93. [[CrossRef](#)]
45. Shen, Y.; Liu, C.; Liu, M.; Zeng, Y.; Tian, C. Change in pan evaporation over the past 50 years in the arid region of China. *Hydrol. Process.* **2010**, *24*, 225–231. [[CrossRef](#)]
46. Zheng, H.; Liu, X.; Liu, C.; Dai, X.; Zhu, R. Assessing contributions to pan evaporation trends in Haihe River Basin, China. *J. Geophys. Res.* **2009**, *114*, 144–153. [[CrossRef](#)]
47. Sen, P. Estimates of the regression coefficient based on Kendall's tau. *J. Am. Stat. Assoc.* **1968**, *63*, 1379–1389. [[CrossRef](#)]
48. Yue, S.; Pilon, P.; Cavadias, G. Power of the Mann-Kendall and Spearman's rho tests for detecting monotonic trends in hydrological series. *J. Hydrol.* **2002**, *259*, 254–271. [[CrossRef](#)]
49. Ma, Q.; Zhang, J.; Sun, C.; Guo, E.; Zhang, F. Mengmeng Wang Changes of reference evapotranspiration and its relationship to dry/wet conditions based on the aridity index in the Songnen grassland, northeast China. *Water* **2017**, *9*, 316. [[CrossRef](#)]
50. Basistha, A.; Arya, D.S.; Goel, N.K. Spatial Distribution of Rainfall in Indian Himalayas—A Case Study of Uttarakhand Region. *Water Resour. Manag.* **2008**, *22*, 1325–1346. [[CrossRef](#)]
51. Gong, L.; Xu, C.; Chen, D.; Halldin, S.; Chen, Y.D. Sensitivity of the Penman-Monteith reference evapotranspiration to key climatic variables in the Changjiang (Yangtze River) basin. *J. Hydrol.* **2006**, *329*, 620–629. [[CrossRef](#)]
52. Zuo, D.; Xu, Z.; Yang, H.; Liu, X. Spatiotemporal variations and abrupt changes of potential evapotranspiration and its sensitivity to key meteorological variables in the Wei River basin, China. *Hydrol. Process.* **2012**, *26*, 1149–1160. [[CrossRef](#)]
53. Liang, L.; Li, L.; Zhang, L.; Li, J.; Li, B. Sensitivity of penman-monteith reference crop evapotranspiration in Tao'er River Basin of northeastern China. *Chin. Geogr. Sci.* **2008**, *18*, 340–347. [[CrossRef](#)]
54. Zhang, X.; Kang, S.; Zhang, L.; Liu, J. Spatial variation of climatology monthly crop reference evapotranspiration and sensitivity coefficients in Shiyang river basin of northwest China. *Agric. Water Manag.* **2010**, *97*, 1506–1516. [[CrossRef](#)]
55. Tang, B.; Tong, L.; Kang, S.; Zhang, L. Impacts of climate variability on reference evapotranspiration over 58 years in the Haihe river basin of north China. *Agric. Water Manag.* **2011**, *98*, 1660–1670. [[CrossRef](#)]
56. Ye, X.; Li, X.; Liu, J.; Xu, C.; Zhang, Q. Variation of reference evapotranspiration and its contributing climatic factors in the Poyang Lake catchment, China. *Hydrol. Process.* **2014**, *28*, 6151–6162. [[CrossRef](#)]
57. Zhang, Y.; Liu, C.; Tang, Y.; Yang, Y. Trends in pan evaporation and reference and actual evapotranspiration across the Tibetan Plateau. *J. Geophys. Res. Atmos.* **2007**, *112*, 1103–1118. [[CrossRef](#)]
58. Cao, W.; Shen, S.; Duan, C. Temporal-spatial variations of potential evapotranspiration and quantification of the causes in Northwest China. *Acta Ecol. Sin.* **2012**, *32*, 3394–3403.
59. Gao, Z.; He, J.; Dong, K.; Bian, X.; Li, X. Sensitivity study of reference crop evapotranspiration during growing season in the West Liao River basin, China. *Theor. Appl. Climatol.* **2016**, *124*, 865–881. [[CrossRef](#)]

60. Zhang, X.; Ren, Y.; Yin, Z.; Lin, Z.; Zheng, D. Spatial and temporal variation patterns of reference evapotranspiration across the Qinghai-Tibetan Plateau during 1971–2004. *J. Geophys. Res.* **2009**, *114*, 4427–4433. [[CrossRef](#)]
61. Xu, M.; Chang, C.; Fu, C.; Qi, Y.; Robock, A.; Robinson, D.; Zhang, H. Steady decline of east Asian monsoon winds, 1969–2000: Evidence from direct ground measurements of wind speed. *J. Geophys. Res.* **2006**, *111*, 906–910. [[CrossRef](#)]
62. Vautard, R.; Cattiaux, J.; Yiou, P.; Thépaut, J.; Ciais, P. Northern Hemisphere atmospheric stilling partly attributed to an increase in surface roughness. *Nat. Geosci.* **2010**, *3*, 756–761. [[CrossRef](#)]
63. Stanhill, G.; Cohen, S. Global dimming: A review of the evidence for a widespread and significant reduction in global radiation with discussion of its probable causes and possible agricultural consequences. *Agric. For. Meteorol.* **2001**, *107*, 255–278. [[CrossRef](#)]
64. Liepert, B. Observed reductions of surface solar radiation at sites in the United States and worldwide from 1961 to 1990. *Geophys. Res. Lett.* **2002**, *29*. [[CrossRef](#)]
65. Stjern, C.W.; Kristjansson, J.E.; Hansen, A.W. Global dimming and global brightening—an analysis of surface radiation and cloud cover data in northern Europe. *Int. J. Climatol.* **2008**, *29*, 643–653. [[CrossRef](#)]
66. Wild, M. Global dimming and brightening: A review. *J. Geophys. Res. Atmos.* **2009**, *114*. [[CrossRef](#)]
67. Wild, M.; Gilgen, H.; Roesch, A.; Ohmura, A.; Long, C.N.; Dutton, E.G.; Forgan, B.; Kallis, A.; Russak, V.; Tsvetkov, A. From dimming to brightening: Decadal changes in solar radiation at Earth’s surface. *Science* **2005**, *308*, 847–850. [[CrossRef](#)] [[PubMed](#)]
68. Norris, J.R.; Wild, M. Trends in aerosol radiative effects over Europe inferred from observed cloud cover, solar “dimming”, and solar “brightening”. *J. Geophys. Res. Atmos.* **2007**, *112*. [[CrossRef](#)]
69. Qian, Y.; Wang, W.; Leung, L.R.; Kaiser, D.P. Variability of solar radiation under cloud-free skies in China: The role of aerosols. *Geophys. Res. Lett.* **2007**, *34*. [[CrossRef](#)]
70. Che, H.Z.; Shi, G.Y.; Zhang, X.Y.; Arimoto, R.; Zhao, J.Q.; Xu, L.; Wang, B.; Chen, Z.H. Analysis of 40 years of solar radiation data from China, 1961–2000. *Geophys. Res. Lett.* **2005**, *32*. [[CrossRef](#)]
71. Zhang, Q.; Xu, C.Y.; Chen, X. Reference evapotranspiration changes in China: Natural processes or human influences? *Theor. Appl. Climatol.* **2011**, *103*, 479–488. [[CrossRef](#)]
72. Roderick, M.L.; Farquhar, G.D. The cause of decreased pan evaporation over the past 50 years. *Science* **2002**, *298*, 1410–1411. [[PubMed](#)]
73. Liu, C.; Zeng, Y. Changes of pan evaporation in the recent 40 years in the Yellow River Basin. *Water Int.* **2004**, *29*, 510–516. [[CrossRef](#)]
74. Li, Y.; Liang, K.; Bai, P.; Feng, A.; Liu, L.; Dong, G. The spatiotemporal variation of reference evapotranspiration and the contribution of its climatic factors in the Loess Plateau, China. *Environ. Earth Sci.* **2016**, *75*, 1–14. [[CrossRef](#)]
75. Xu, Y.; Xu, Y.; Wang, Y.; Wu, L.; Li, G.; Song, S. Spatial and temporal trends of reference crop evapotranspiration and its influential variables in Yangtze River Delta, eastern China. *Theor. Appl. Climatol.* **2016**, 1–14. [[CrossRef](#)]
76. He, Y.; Ye, J.; Yang, X. Analysis of the spatio-temporal patterns of dry and wet conditions in the Huai River Basin using the standardized precipitation index. *Atmos. Res.* **2015**, *166*, 120–128. [[CrossRef](#)]

